Ultraviolet Resonance Raman Spectroscopy of the Nucleotides with 266-, 240-, 218-, and 200-nm Pulsed Laser Excitation

Stephen P. A. Fodor, Richard P. Rava, Thomas R. Hays, and Thomas G. Spiro*

Contribution from the Department of Chemistry, Princeton University, Princeton, New Jersey 08544. *Received July 3, 1984*

Abstract: Ultraviolet resonance Raman spectra are reported for the deoxyribonucleotides of uracil, thymine, cytosine, guanine, and adenine (dUMP, dTMP, dCMP, dGMP, and dAMP) in dilute (5×10^{-3} M) aqueous solution. Excitation (266, 240, 218, and 200 nm) was generated with a frequency-quadrupled Nd:YAG laser (266 nm) and a H_2 Raman shifter operated at the first, second, and third anti-Stokes lines. The spectra contain vibrational bands due to the in-plane modes of the purine and pyrimidine rings and show large alterations among the four wavelengths in the enhancement patterns. These changes are helpful in resolving overlapped bands and making assignments (e.g., of the dUMP C4=O and C2=O stretches, at 1674 and 1686 cm^{-1}). The enhancements are discussed in the light of mode assignments (from previous normal coordinate calculations) and the character of the excited states, as deduced from previous CNDO calculations. For dUMP and dTMP the enhancements are interpreted in terms of resonance with electronic transitions based on the C6=C5—C4=O and C2=O fragments at long and short wavelengths, respectively. However, the strengths of bands at 1230 (dUMP) and 1244 (dTMP) cm^{-1} are anomalous and suggest a need for normal mode revisions. For dGMP and dAMP, the intensities are consistent with a N7=C8 localized transition at long wavelengths and a series of triene-based transitions throughout the UV region. An instance of vibronic (*B* term) enhancement is suggested for dGMP, in resonance with a weak transition at 215 nm. RR spectra are reported for an equimolar mixture of dTMP, dCMP, dGMP, and dAMP, and the major contributors are identified at each wavelength. The enhancement variations give promise for isolating the key bands associated with the individual bases in RR spectra of nucleic acids.

Introduction

Heightened interest in the molecular mechanisms of gene expression places great importance on structural probes of the nucleic acids. Among the applicable techniques, resonance Raman spectroscopy offers the structural specificity associated with molecular vibrational frequencies, and the sensitivity and selectivity provided by resonance enhancement.[1-3] When the sample is excited at wavelengths near allowed electronic transitions of the molecules, large enhancements of the scattered light are seen for vibrations associated with the chromophore. The purine and pyrimidine bases of the nucleic acids absorb strongly at wavelengths shorter than 280 nm. Until now, this region of the spectrum has not been readily accessible because of laser source limitations. While much progress has been made in Raman studies of nucleic acids with visible laser excitation,[4-8] these studies are hampered by low sensitivity and selectivity. High sample concentrations are required, and the overlap of Raman bands associated with different nucleic acid constituents is a serious hindrance to spectral interpretation.

The promise of high sensitivity and selective enhancement has spurred efforts to obtain UV-excited Raman spectra. Excitation in or near the first strong nucleotide absorption bands has been possible via frequency doubling of the 514.5-nm output of the Ar^+ laser[9,10] or with pulsed dye lasers.[11,12] The advent of the pulsed Nd:YAG laser opens a much wider region of the ultraviolet spectrum for RR studies, because the high pulse energies and well-defined pulse shapes allow efficient wavelength shifting through nonlinear optical processes. The fourth harmonic, at 266 nm, is well matched to the first allowed transitions of the purine and pyrimidine bases, and shorter wavelengths can readily by generated[13,14] in order to probe higher lying transitions. Ziegler et al.[15] have recently demonstrated that marked intensity changes are observed for nucleotide RR spectra excited at 266 and 213 nm, the latter wavelength being the fifth harmonic of the YAG laser, generated with a low-temperature (-40 °C) KDP crystal.[13]

In this work we have used an H_2 Raman shift cell[16] to convert the 266-nm YAG output to shorter wavelengths, by multiples of the 4155-cm^{-1} H_2 stretching frequency. High-quality spectra have been obtained in this manner for the deoxyribonucleotides of uracil, thymine, cytosine, guanine, and adenine (dUMP, dTMP, dCMP, dGMP, and dAMP) with 266, 240, 218, and 200 nm. The spectra are rich in detail and reveal new vibrational features which have not previously been resolved. Dramatic changes in enhancement patterns are observed among the four excitation lines, reflecting the fact that a number of different electronic transitions become resonant at these wavelengths. The assignments of these transitions are far from secure,[17] and the RR enhancements can be expected to play an important role in elucidating the purine and pyrimidine electronic spectra, since the RR intensities are directly related to the nature of the excited states.[18]

At a practical level, the variations in the enhancement patterns for the different bases give promise for disentangling their spectral contributions through variable wavelength excitation. We report RR spectra of a mixture of nucleotides, which demonstrate that

(1) See: Carey, P. R. "Biochemical Application of Raman and Resonance Raman Spectroscopies"; Academic Press: New York, 1982.
(2) Spiro, T. G.; Gaber, B. P. *Annu. Rev. Biochem.* **1977**, *46*, 553.
(3) Spiro, T. G.; Stein, P. *Annu. Rev. Phys. Chem.* **1977**, *28*, 501.
(4) Brown, E. B.; Peticolas, W. L. *Biopolymers* **1975**, *14*, 1259.
(5) Tsuboi, M.; Takahushi, S.; Harada, I. In "Physico-chemical Properties of Nucleic Acids"; Duchesne, J., Ed.; Academic Press: New York, 1973; Vol. 2, p 91.
(6) Hartman, K. A.; Lord, R. C.; Thomas, G. J., Jr. In ref 5, p 1.
(7) Thamann, T. J.; Lord, R. C.; Wang, A. H. T.; Rich, A. *Nucl. Acids Res.* **1981**, *9*, 5443.
(8) Wartell, R. M.; Klysik, J. E.; Hillen, W.; Wells, R. D. *Proc. Natl. Acad. Sci. U.S.A.* **1982**, *79*, 2549.
(9) Nishimura, Y.; Hirakawa, A. Y.; Tsuboi, M. *Adv. Infrared Raman Spectrosc.* **1979**, *5*, 217.
(10) Chinsky, L.; Turpin, P. Y. *Biopolymers* **1982**, *21*, 277.
(11) (a) Chinsky, L.; Laigle, A.; Peticolas, W. L.; Turpin, P. Y. *J. Chem. Phys.* **1982**, *76*, 1. (b) Chinsky, L.; Turpin, P. Y.; Duquesne, M.; Brahms, J. *Biopolymers* **1977**, *17*, 1347.
(12) (a) Blazej, D. C.; Peticolas, W. L. *Proc. Natl. Acad. Sci. U.S.A.* **1977**, *74*, 2639. (b) Blazej, D. C.; Peticolas, W. L. *J. Chem. Phys.* **1980**, *72*, 3134.
(13) Ziegler, L. D.; Hudson, B. *J. Chem. Phys.* **1981**, *74*, 982.
(14) Asher, S. A.; Johnson, C. R.; Murtaugh, J. *Rev. Sci. Instrum.* **1983**, *54*, 1657.
(15) Ziegler, L. D.; Hudson, B.; Strommen, D. P.; Peticolas, W. L. *Biopolymers* **1984**, *23*, 2067.
(16) Wilke, W.; Schmidt, W. *Appl. Phys.* **1979**, *18*, 177.
(17) Callis, P. R. *Annu. Rev. Phys. Chem.* **1983**, *34*, 329.
(18) Peticolas, W. L.; Strommen, D. P.; Lakshminarayanan, V. *J. Chem. Phys.* **1980**, *73*, 4185, and references therein.

0002-7863/85/1507-1520$01.50/0

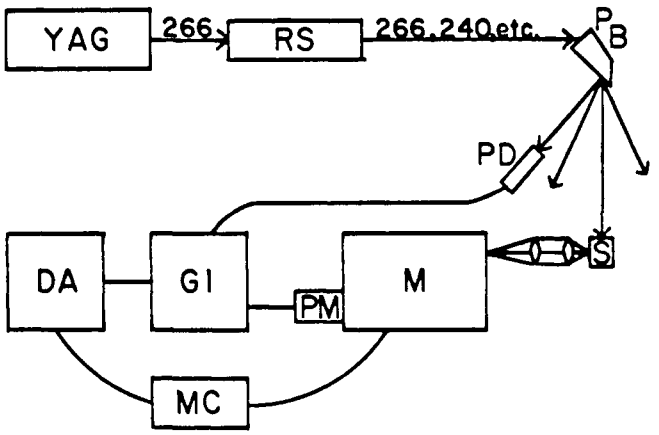

Figure 1. Schematic of experimental setup. YAG, Nd^{3+}:YAG laser; RS, hydrogen-filled Raman shifting cell; PB, Pellin–Broca dispersing prism; S, sample; M, monochromator; PM, photomultiplier tube; GI, gated integrator; DA, data acquisition and control computer; MC, monochromator control unit; PD, trigger photodiode.

by judicious choice of the laser wavelength one can discriminate among the bases with respect to most of the vibrational modes of interest.

Experimental Section

All of the mononucleotides were the highest grade disodium salt form available from Sigma, and were used without further purification.

Figure 1 summarizes the main elements of the experimental arrangement. The excitation source was the 266-nm fourth harmonic line from a Nd^{3+}:YAG laser (DCR-1A or DCR-2A, Quanta-Ray). For the higher frequency lines, this was focused into a home-built, 100-cm long hydrogen shifting cell[16] operated at 3.3 atm. The various Raman-shifted lines were dispersed by means of a Pellin-Broca prism, and the desired line was focused onto the sample. To avoid problems with sample cell fluorescence and damage, and accumulation of photoproducts on cell walls, the beam intersected the sample in the free jet portion of a recirculating flow system.[13] In general, 2 to 10 mL of sample was recirculated by a peristaltic pump to form a jet about 1 mm diameter; 120° backscattering collection geometry was employed.

In order to compare the nucleotide Raman intensities at different excitation wavelengths, the O–H stretching band of the water solvent molecules was used as an internal standard. The molar scattering ratio for a given nucleotide band was calculated from the following expression:

$$\frac{\sigma_N}{\sigma_{H_2O}} = \frac{I_N C_{H_2O}}{I_{H_2O} C_N}\left[\frac{(\epsilon_N\chi + \epsilon_0)(1 - \exp(-2.3C_N l/(\epsilon_{H_2O}\chi + \epsilon_0))}{(\epsilon_{H_2O}\chi + \epsilon_0)(1 - \exp(2.3C_N l/(\epsilon_N\chi + \epsilon_0)}\right]$$

$$\chi = \sin\left[\cos^{-1}\left(\frac{n_1}{n_2}\cos\theta\right)\right] \quad (1)$$

where I_N/I_{H_2O} is the measured peak height ratio and C_N/C_{H_2O} is the molar concentration ratio (C_{H_2O} = 55.5 M). The term in square brackets is a correction for self-absorption;[19,20] ϵ_0, ϵ_N, and ϵ_{H_2O} are the molar absorptivities at the laser wavelength, and at the wavelengths of the nucleotide and H_2O Raman bands, respectively; l is the diameter of the sample jet; n_1 and n_2 are refractive indexes for air and for the sample; θ is the angle between the laser beam and the sample surface (30° in our experiment; χ accounts for the differing paths of the incident and scattered photons). Because of the large frequency differences between the nucleotide and H_2O bands, the absorption correction is appreciable, ranging up to factors of 10 under our conditions.

The spectrometer response function was obtained using an Optronic Laboratories Model UV-40 ultraviolet irradiance standard calibrated from 180 to 400 nm.

Results

Figure 2 is a structural diagram for the purine and pyrimidine bases of the five deoxynucleotides included in this study, with the conventional atom numbering scheme. Figure 3 is a summary of the electronic absorption spectra for uracil, thymine, cytosine, guanine, and adenine, taken from a recent review of the data by Callis.[17] Underneath the dotted absorption curves, the positions and strengths of the currently assigned electronic transitions are given by solid bars, with flags indicating the direction of polarization relative to the molecular axes shown. Arrows mark the position of the four laser lines (266, 240, 218, and 200 nm), used in this study.

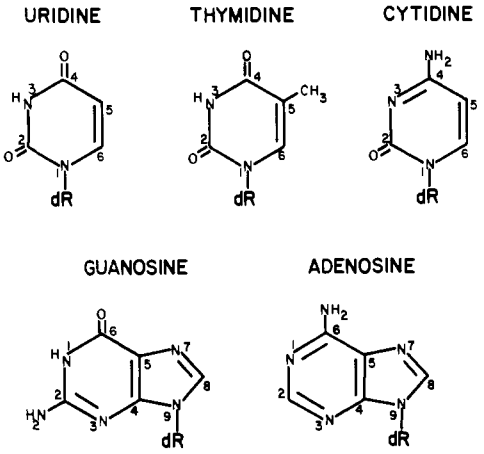

Figure 2. Structures and numbering conventions for the deoxyribonucleotides.

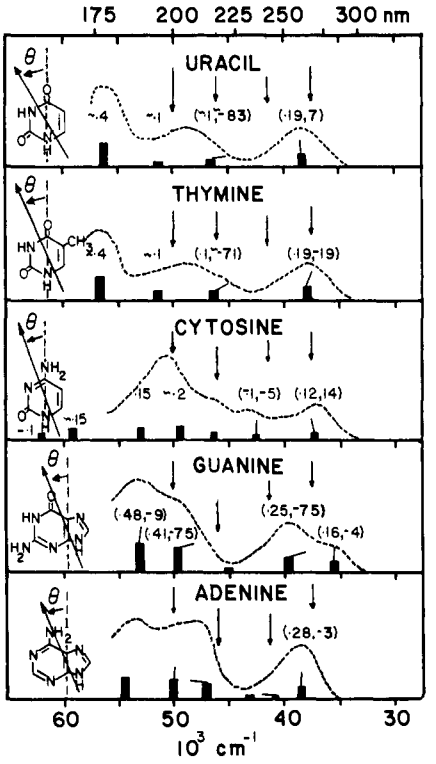

Figure 3. Ultraviolet absorption spectra for the five mononucleotides adapted from ref 17. Estimated oscillator strengths and transition polarizations are given in parentheses. The same information is displayed graphically by height and direction of block and tilted arrow, respectively. The DeVoe–Tinoco convention for transition polarization is used and illustrated to the left of each spectrum. Vertical arrows indicate the laser frequencies utilized in this study.

RR spectra at 266, 240, 218, and 200 nm are shown in Figures 4–8 for the five nucleotides in dilute (5×10^{-3} M) aqueous solution. These spectra have all been normalized via the intensity of the ~3400-cm^{-1} O–H stretching band of the solvent water. Appreciable resonance enhancement is not expected for the water band itself. (The first water absorption band is 150 nm.[21]) It

(19) Shriver, D. F.; Dunn, J. B. R. *Appl. Spectrosc.* **1974**, *28*, 319.
(20) Strekas, T. C.; Adams, D, H.; Parker, A.; Spiro, T. G. *Appl. Spectrosc.* **1974**, *28*, 324.
(21) Heller, J. M., Jr.; Hamm, R. N.; Birkhoff, R. D.; Painter, L. R. *J. Chem. Phys.* **1974**, *60*, 3483.

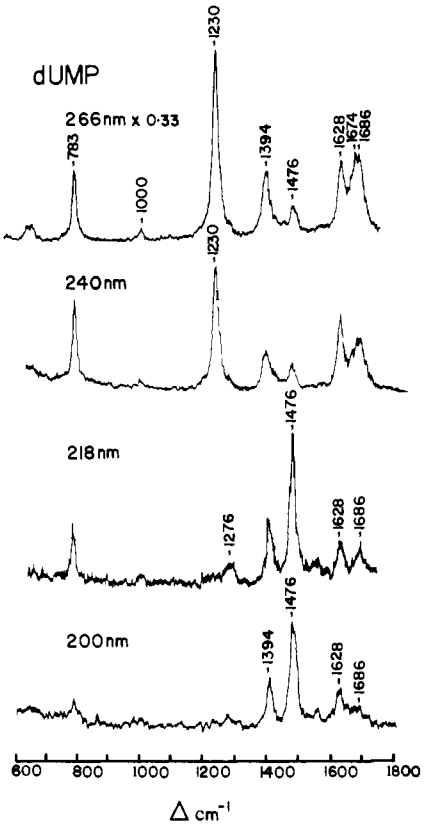

Figure 4. Resonance Raman spectra of aqueous deoxyuridine 5′-monophosphate (5 mM) with 266-, 240-, 218-, and 200-nm excitation. All spectra have been scaled relative to the intensity of the 3400-cm^{-1} O–H water stretching band. The intensity of the 266-nm spectrum has been multiplied by 0.33.

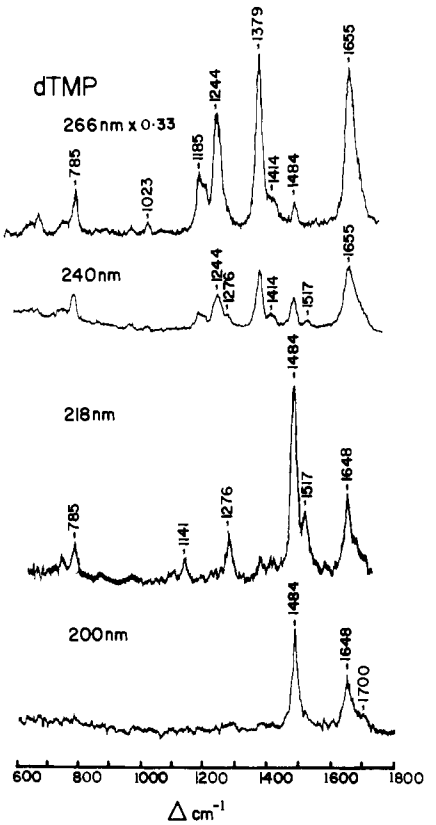

Figure 5. Resonance Raman spectra as in Figure 4 of aqueous (5 mM) deoxythymidine 5′-monophosphate. The intensity of the 266-nm spectrum has been multiplied by 0.33.

is clear that 266-nm excitation gives the strongest enhancement for all of the nucleotides. The lower overall enhancement at the other wavelengths is also accompanied by substantial relative intensity changes among the individual bands. Table I gives enhancement values for the prominent RR bands.

Figures 9–13 show the effects of dissolving the nucleotides in D_2O on the RR spectra taken at 266 and 218 nm. For dUMP and dTMP, the only exchangeable proton (aside from those of the ribose ring, which are not expected to have any significant effect on the enhanced base modes) is on the ring N3 atom. The profound effects which are observed reflect extensive couplings of the N3–H bending coordinate with the ring modes. Neither dCMP nor dAMP have exchangeable protons on any of the ring atoms, and the effects which are seen must be associated with exchange of the exocyclic NH_2 protons. dGMP has exchangeable protons on both ring (N1) and exocyclic N atoms. Figure 14 shows spectra at the four excitation wavelengths of an equimolar mixture of dTMP, dCMP, dGMP, and dAMP. The main contributors to the observed bands are indicated by the appropriate letters.

Discussion

A. Assignments. All of the Raman bands are attributable to vibrational modes of the heterocyclic bases, whose electronic transitions are responsible for the resonance enhancement. At the low concentrations (5×10^{-3} M) used, Raman bands associated with sugar or phosphate vibrations are not expected to be seen, and none have been identified. Band frequencies are listed in Table II, along with suggested mode correspondences calculated by Tsuboi et al.[5] for the 1-methylpyrimidine and 9-methylpurine bases. These correspondences are based on approximate frequency matching, deuteration shifts, and consideration of the nature of the resonant excited state (see section B).

1. Exocyclic C=O and C—NH_2 Modes. An important feature of the variable wavelength excitation is that overlapping bands can often be resolved via their different enhancement patterns.

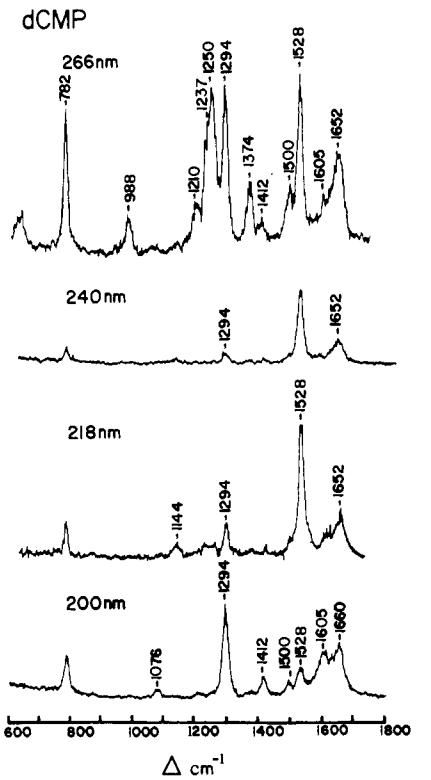

Figure 6. Resonance Raman spectra as in Figure 4 of aqueous (5 mM) deoxycytidine 5′-monophosphate.

For instance, the dUMP 266-nm spectrum (Figure 4) shows a broad band centered at 1680 cm^{-1}, also seen via visible excitation,[22]

(22) Lord, R. C.; Thomas, G. J., Jr. *Spectrochim. Acta, Part A* **1967**, *23*, 2551.

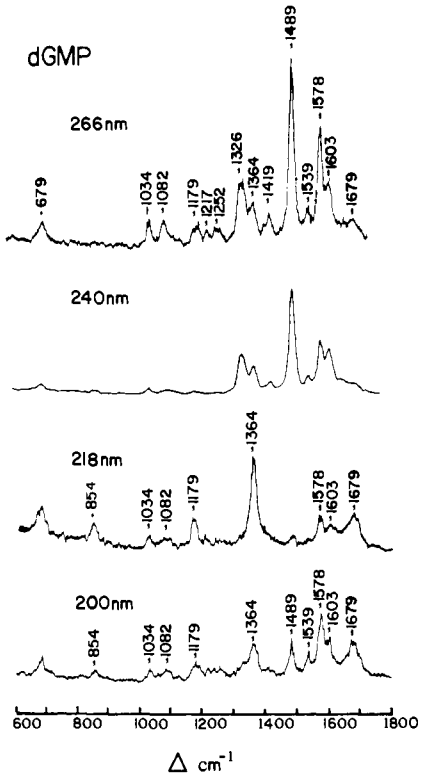

Figure 7. Resonance Raman spectra as in Figure 4, of aqueous (5 mM) deoxyguanine 5′-monophosphate.

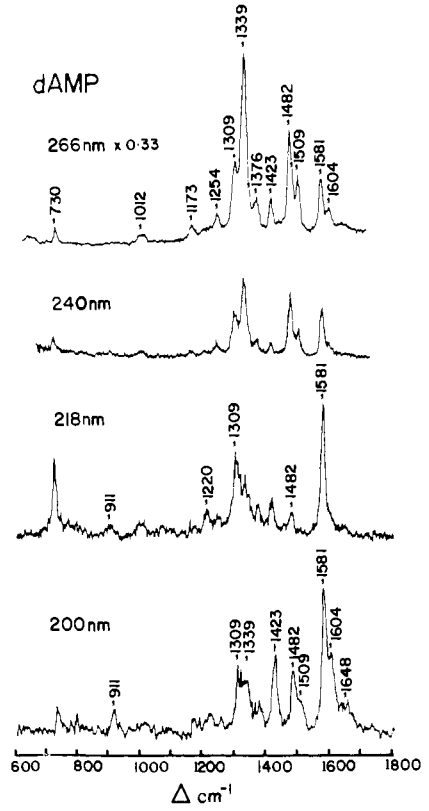

Figure 8. Resonance Raman spectra as in Figure 4, of aqueous (5 mM) deoxyadenine 5′-monophosphate. The intensity of the 266-nm spectrum has been multiplied by 0.33.

which is believed to contain both of the C=O stretches because of its sensitivity to ^{18}O substitution at either C4 or C2.[23] In the 218-nm spectrum, however, a narrower band is seen at 1686 cm^{-1}, and is assignable primarily to the C2=O stretch, since the resonant electronic transition (215 nm, Figure 3) is polarized in the direction

Table I. Molar Enhancement Factors[a] ($\times 10^{-2}$) Relative to the 3400-cm^{-1} H_2O Band for Selected Nucleotide RR Bands

λ_0, nm	mode		
	dUMP		
	1628 cm^{-1}	1476 cm^{-1}	1230 cm^{-1}
266	153	44	380
240	35	12	59
218	33	107	
200	33	90	
	dTMP		
	1484 cm^{-1}	1379 cm^{-1}	
266	38	319	
240	12	25	
218	122		
200	78		
	dCMP		
	1528 cm^{-1}	1294 cm^{-1}	
266	214	210	
240	80	15	
218	206	53	
200	75	204	
	dGMP		
	1578 cm^{-1}	1489 cm^{-1}	1364 cm^{-1}
266	217	384	75
240	80	202	48
218	40	18	132
200	176	111	101
	dAMP		
	1581 cm^{-1}	1482 cm^{-1}	1339 cm^{-1}
266	277	554	956
240	68	85	101
218	222	29	92
200	321	134	113

[a] See Experimental Section for details of the calculation.

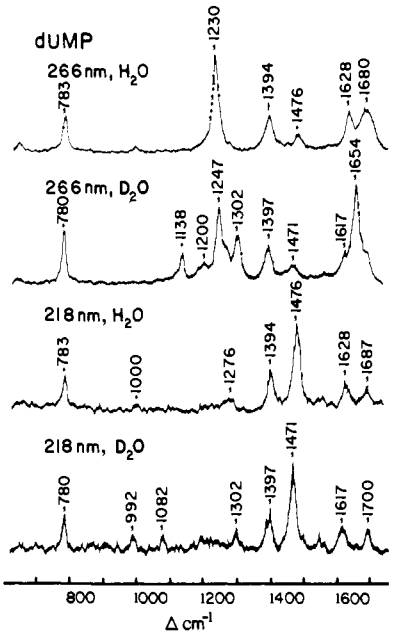

Figure 9. Resonance Raman spectra of 5 mM deoxyuridine 5′-monophosphate in H_2O and D_2O with 266- and 218-nm laser excitation.

of this bond. Thus the higher energy component of the composite band seen at 266 nm is due to νC2=O, and the lower one (~1674 cm^{-1}) to νC4=O. Chinsky et al.[23] decomposed this band in the 257-nm RR spectrum using ^{18}O substitution at C2 and C4 and deconvolution techniques. They found it necessary to invoke four components, in addition to the adjacent 1628-cm^{-1} band (which appeared only as a shoulder in their spectra). There is no physical

(23) Chinsky, L.; Hubert-Habart, H.; Laigle, A.; Turpin, P. Y. *J. Raman Spectrosc.* **1983**, *14*, 322.

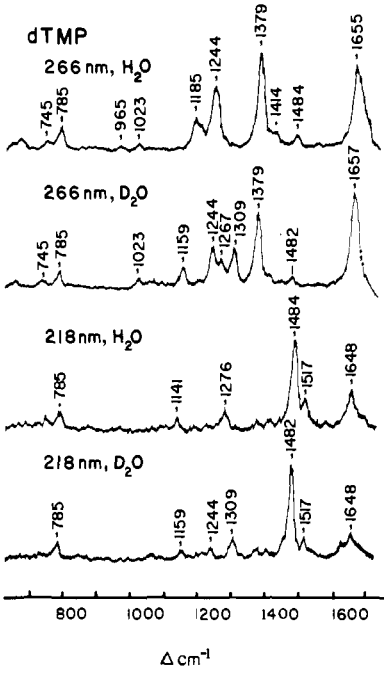

Figure 10. Resonance Raman spectrum of 5 mM deoxythymidine 5′-monophosphate in H_2O and D_2O with 266- and 218-nm laser excitation.

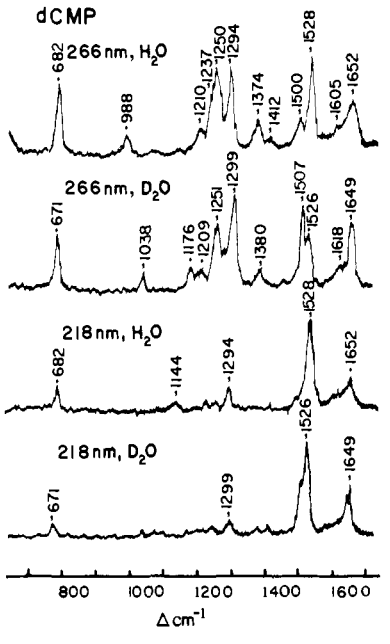

Figure 11. Resonance Raman spectra of 5 mM deoxycytidine 5′-monophosphate in H_2O and D_2O with 266- and 218-nm laser excitation.

reason, however, for expecting so many modes in this region, and the variable wavelength excitation seems a more reliable basis for assigning the C2 and C4 contributions. The band at 1628 cm^{-1}, which is also sensitive to ^{18}O substitution,[23] is assigned to the C5═C6 stretch, coupled to νC4═O (Table II). In dTMP (Figure 5), not only νC2═O and νC4═O, but also νC5═C6 are all overlapped, a single broad band appearing at 1655 cm^{-1} in the 266-nm spectrum. In the 218-nm spectra, however, a narrower band is seen at 1648 cm^{-1}, with a shoulder at 1700 cm^{-1}, which, by analogy with the enhancement pattern seen at 218 nm for dUMP, can be assigned to νC5═C6 and νC2═O, respectively. νC4═O must then be the central component of the 1655-cm^{-1} composite band of the 266-nm spectrum. These assignments are summarized in Table III.

When dUMP is dissolved in D_2O (Figure 9), it can be seen from the 218-nm spectrum that νC2═O and νC5═C6 shift up and down, respectively, to 1700 and 1617 cm^{-1}. In the 266-nm

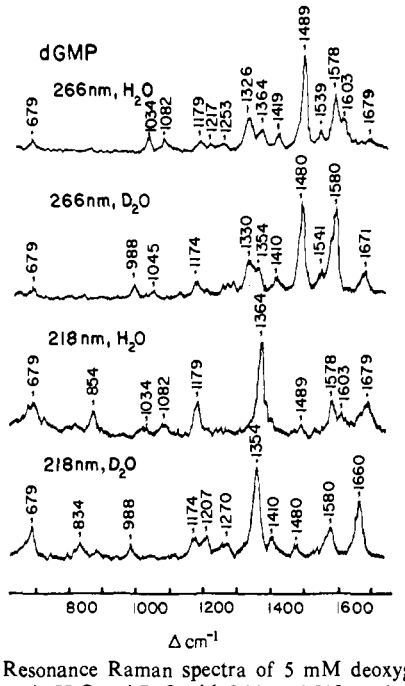

Figure 12. Resonance Raman spectra of 5 mM deoxyguanosine 5′-monophosphate in H_2O and D_2O with 266- and 218-nm laser excitation.

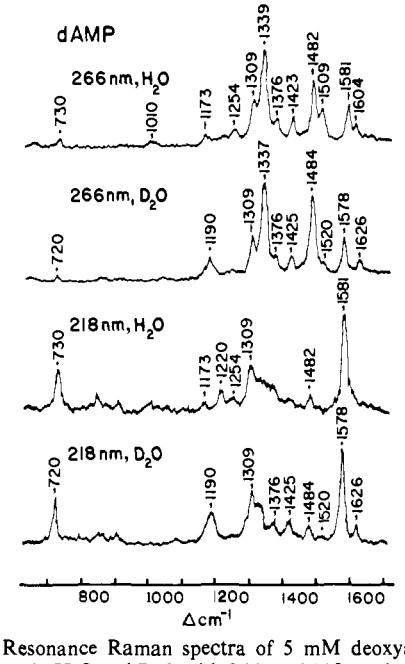

Figure 13. Resonance Raman spectra of 5 mM deoxyadenosine 5′-monophosphate in H_2O and D_2O with 266- and 218-nm laser excitation.

spectrum these bands appear as shoulders flanking a very strong central component at 1654 cm^{-1}, assigned to νC4═O. These effects are associated with the loss of coupling with the N3–H bending coordinate, due to the large decrease in its natural frequency when D replaces H. The uncoupling produces an upshift in νC2═O (1686 → 1700 cm^{-1}), downshifts in νC5═C6 and νC4═O (1628 → 1617 cm^{-1}, 1676 → 1654 cm^{-1}), and an intensification of νC4═O at 266 nm. These frequency assignments are consistent with the results of infrared studies of uridine in D_2O.[24] Interestingly, the dUMP νC═O frequencies in D_2O are similar to the corresponding dTMP frequencies in H_2O; one effect of the methyl substitution at the C5 atom of dTMP appears to be to decouple the C═O stretching modes from N3—H bending (perhaps because the C5—H bending coordinate is also lost). Consistent with this view is the absence of significant changes in the νC═O bands when dTMP is dissolved in D_2O (Figure 10).

(24) Miles, H. T. *Proc. Natl. Acad. Sci. U.S.A.* **1964**, *54*, 1104.

Table II. Nucleotide Raman Bands and Assignments

obsd. frequency (cm^{-1})	rel intensity at λ_0 (nm) 436	266[b]	218[b]	calcd frequency (cm^{-1})[c]	potential energy distribution[c,d]
			A. Uridine (dUMP) in H_2O: 1-Methyluracil		
1686			2	1710	-C2O (47) + C2N3 (24) + δN3H (18)
1674	5	4	1	1651	C5C4 (34) - C4O (34)
1628	2	3	2	1562	N3C4 (22) + N1C2 (21) + C6C5 (20) - N1C6 (19)
1476	1	1	10	1491	-N1C2 (38) + C2N3 (17)
1394	4	3	3	1375	-δN3H (48) - C4O (27)
1276			1		
1230	10	10	0	1200	-δC6H (23) + C2N3 (15)
1000	1	1	0	1009	-δC6H (45) + C5C4 (10)
783	3	3	4	826	N1C2 (14) + N1R (10) + C5C4 (10) + N1C6 (9) + N3C4 (8)
			B. Uridine (UMP) in D_2O: 1-Methyluracil		
1700	6		2	1691	C2O (63) - C2N3 (22)
1654	10	10	0	1644	C5C4 (34) - C4O (37)
1617	3	3	2		
1471	1	1	10	1481	-N1C2 (33) + N3C4 (21)
1397	4	4	5		
1302	5	5	2	1299	N1C6 (27) + C5C6 (22)
1247	9	8	0	1258	-C4O (23) + δ3D (12) + C2O (11) - δC6H (10)
1200	2	2	1		
1138	3	3	0	1124	N1R (45) - δC5C6N1 (7) + δC6N1C2 (7) - δC5H (7)
992	3	0	2		
780	5	6	5	821	N1C2 (13) + C5C4 (10) + N1C6 (9) + N3C4 (7)
			C. Cytosine (dCMP):[e] 1-Methylcytosine		
1660				1588	C4C5 (38) + δNH2 (29)
1652 (-3)	1 (2)	7 (6)	4 (5)	1652	C2O (67) - C2N3 (15)
1605	2 (3)	1 (2)	1 (0)	1630	δNH2 (58) + C4N4′ (19)
1528	6 (4)	10 (5)	10	1538	-N3C4 (38) - N1C2 (14)
1500 (+7)	0 (4)	3 (8)	0 (6)	1521	-N1C2 (38) + N1C6 (34) + C2N3 (27)
1412	0 (1)	1 (0)	0 (1)		
1374 (+5)	1	3 (2)	0	1443	C4N4′ (29) + N1C2 (16)
1294 (+6)	10	10	2 (1)	1320	N1C6 (28) + C5C6 (19)
1250	10 (5)	10 (7)	1	1212	δC6H (31) + C4N4′ (19)
1237					
1210	4 (3)	0 (2)			
1144		0 (0)	1 (0)		
988 (+49)	2 (3)	3	0	1037	NH_{2rock} (36) + δC6H (24)
782 (-11)	9 (8)	7 (5)	2	768	N1R (18) - C4N (14) - C4C5C6 (13)
			D. Guanine (dGMP): 9-Methylguanine		
1679 (-8)	3	1 (3)	4 (7)	1692	C6O (48) - C5C6 (21) + C5C4 (11) + δN1H (11) - N1C6 (10)
1679 (-18)					
1603	3 (1)	2 (0)	0	1615	δNH_2 (83) + C2N2′ (15)
1579	8 (10)	5 (10)	3 (3)	1592	-C4N3 (30) + C5C4 (24) - N7C5 (16)
1539	1 (3)	1	0	1432	-C4N9 (33) - N7C5 (24)
1489 (-9)	10 (5)	10 (10)	1	1459[f]	δC8H (40) - N9C8 (32) + C8N7 (21)
1419 (-8)	2	1	0		
1364 (-11)	4 (3)	2 (3)	10 (10)	1290	-C8N7 (26) - N1C6 (25) + N7C5 (16)
1326 (+3)	3	3	0	1198[g]	-δC8H (25) + C8N7 (19)
1253		1 (0)	0 (1)		
1217		1 (0)	0 (1)		
1179 (-5)	2 (1)	1	3 (2)		
1082 (-37)	2 (0)	1	1		
1034 (-45)					
854 (-20)	2 (1)	1	2	965	-N9R (16) + N3C2 (13)
679	2	1	3	684	δN7C8N9 (15) + δC5N7C8 (15)
			E. Adenine (dAMP):[a] 9-Methyladenine		
1649 (-22)	0	0 (1)		1623	C5C6 (48) + δNH2 (20)
1604	0	1 (0)	0	1647	δNH_2 (73) - C5C6 (15) + C6N6′ (14)
1581 (-3)	7 (6)	4	10	1581	C5C4 (48) - C4N3 (31)
1509 (+9)	3 (2)	3 (0)	0		
1482	3 (4)	6 (9)	2	1468[h]	-δC2H (29) - N9C8 (19) + δC8H (15)
1423 (+2)	2 (1)	2	3	1489[i]	C4N9 (44) - δC8H (15)
1376	4 (3)	2	1	1424	
1339	10	10	4	1329	-N7C5 (39) + C8N7 (12)
1309	7	4	6	1309	N9C8 (30) + N3C2 (14) + δC8H (14) - δC2H
1254	2	1	1	1424	-N1C6 (31) + C6N6′ (26)
1220					
1173	0	1 (3)	1 (3)		
1012 (+29)	0	0	1		
730 (-10)	3	1	6	681	-δN7C8N9 (19) - N9R (14) + δC5N7C8 (12) + C4N9C8 (11)

[a] Taken from ref 22. [b] Present work. [c] From ref 5. [d] Percent contributions (in parentheses) from bond stretching or bending (δ) coordinates; minor contributors are not listed, prime designates exocyclic atom [e] Values in parentheses are frequency shifts (cm^{-1}) or relative intensities for dCMP in D_2O. [f] Shifts down 28 cm^{-1} on C8 deuteration.[27a] [g] Shifts down 15 cm^{-1} on imidazole N^{15} and 17 cm^{-1} on C8 deuteration.[26,27] [h] Shifts down 23 cm^{-1}

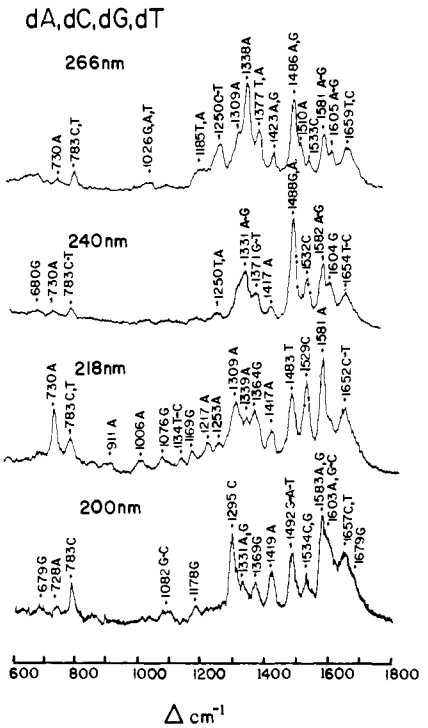

Figure 14. Resonance Raman spectra of an aqueous solution containing 1 mM each of dAMP, dCMP, dGMP, and dTMP with 266-, 240-, 218-, and 200-nm laser excitation. Letters identify the bases making the dominant contributions to the indicated bands (see text).

Table III. Summary of Assignments for Exocyclic and High-Frequency C=C Modes (cm^{-1}) of the Nucleotides

	C2=O	C4=O	C=C	δNH_2	C—NH_2
dUMP in H_2O	1686	~1674	1628		
in D_2O	1700	1654	1617		
dTMP in H_2O	~1700	1655	1648		
in D_2O	~1700	1657	1648		
dCMP in H_2O	1652		1660	1605	~1237
in D_2O	1649		1618	1176	
	(C6=O)				
dGMP in H_2O	~1679		1679	1603	
in D_2O	1671		1660	1207	
dAMP in H_2O			1648	1604	1254
in D_2O			1626	1190	

dAMP, which has no C=O substituent, shows a band at 1648 cm^{-1} in H_2O (200 nm, Figure 8) and 1626 cm^{-1} in D_2O (Figure 13). Since the six-membered ring of adenine is aromatic, this band may be related to a high-frequency ring mode of substituted benzenes, ν_{8b}, which is generally coupled to the substituents.[25] Both dCMP and dGMP have a single C=O substituent, whose stretch is expected in this region, but they also show an additional band, which is presumably a C=C stretching mode. In dGMP only one band is apparent at 1679 cm^{-1} in H_2O, but the existence of two bands is evidenced by the different frequencies, 1671 and 1660 cm^{-1}, seen for the highest frequency bands in the 266- and 218-nm D_2O spectra (Figure 12). These are assigned to C6=O and C5=C4 stretching, by analogy with dUMP. dCMP shows a single prominent band at 1652 cm^{-1} (Figure 6) at all wavelengths except 200 nm, where a high-frequency shoulder appears (~1660 cm^{-1}). In D_2O (Figure 11), on the other hand, a strong band at 1649 cm^{-1} has a low-frequency shoulder, at 1618 cm^{-1}. Since the only exchangeable protons on C are at the NH_2 group, and should not affect νC=O strongly, we assign νC=O to the prominent bands at 1652 cm^{-1} in H_2O and 1649 cm^{-1} in D_2O. The strongly D_2O sensitive band at 1660 cm^{-1} (→1618 cm^{-1}) is assigned to a coupled N3=C4, C5=C6 stretch (though no calculated normal coordinate fits this character (Table II)).

The bases with exocyclic NH_2 groups, C, G, and A, all show bands at ~1605 cm^{-1}, which are assignable to the NH_2 scissors mode,[5] since they disappear in D_2O (Figures 11–13). In D_2O, new bands appear at 1190, 1176, and 1207 cm^{-1} for dAMP, dCMP, and dGMP, respectively. We tentatively assign these modes to the exocyclic ND_2 scissoring as suggested by the normal coordinate analyses (Table II).[5] These bands, which are of great interest in connection with H-bonding interactions of the NH_2 groups, are not resolved in Raman spectra obtained with visible excitation,[22] but are readily seen in the RR spectra, particularly at 200 nm, where they become prominent for all three bases.

One other exocyclic mode that can be identified qualitatively is the C–NH_2 stretch, which is expected to be perturbed upon H/D exchange. At 266 nm, CMP shows a ~1237-cm^{-1} shoulder on its 1250-cm^{-1} band, which disappears in D_2O (Figure 11). Likewise dAMP (Figure 13) has a D_2O-sensitive band at 1254 cm^{-1}. We tentatively assign these bands to νC–NH_2, recognizing that they may have appreciable contributions from ring coordinates. For dGMP, which should have a similar mode, the effect of D_2O on this region of the spectrum is complex, presumably because the N3 proton is also exchanged (see below).

2. Ring Vibrations. The remaining modes are complex mixtures of ring bond stretching and bending coordinates, with substantial contributions from C–H and N–H bending, and qualitative assignments are of limited utility. For dTMP, strong bands at 1484 (218 nm) and 1379 cm^{-1} (266 nm) involve out-of-phase stretches of the ring bonds which are coupled to the C2 and C4 carbonyls, respectively, based on their selective enhancements at short and long wavelengths (see below). For dUMP, however, a 1394-cm^{-1} band corresponding to the 1379-cm^{-1} dTMP band is moderately enhanced at all wavelengths, and the mode composition is inferred to be more distributed around the ring, probably analogous to the bond alternant mode of benzene, ν_{14}, at 1310 cm^{-1}.[25] For dCMP, strong bands at 1528 (218 nm) and 1294 cm^{-1} (266 nm) probably have major contributions from the enimine bonds N3=C4—C5=C6. A shift in intensity in D_2O from the 1528-cm^{-1} band to a neighboring band at 1507 cm^{-1} (Figure 11) implies substantial involvement of the NH_2 group, as well.

For all three pyrimidines, the 1100–1300-cm^{-1} region is very complex and must involve a subtle blend of internal coordinate contributions. This is seen most dramatically in the dUMP 266-nm RR spectra (Figure 9), in which the single strong band at 1230 cm^{-1} is replaced in D_2O by five moderate intensity bands, spread between 1138 and 1302 cm^{-1}. A similar effect is seen with visible excitation.[22] The single replacement of D for H at the N3 atom evidently produces a profound alteration in the normal mode compositions in this region. All of the pyrimidines show a relatively strong band at ~785 cm^{-1}, which can be assigned to the ring breathing mode analogous to the ν_1 mode of benzene at 992 cm^{-1}.[25]

The vibrational patterns for the purines are further complicated by variable contributions from the fused pyrimidine and imidazole rings, which have to some extent been sorted out via isotope studies.[26] The ring modes seen for dAMP and dGMP at 730 and 679 cm^{-1} are apparently localized in the imidazole region.[5] The 679-cm^{-1} band of guanine is of special interest since it is a marker for the $B \rightarrow Z$ conformational switch of alternating dGdC DNA sequences;[7] this conformational sensitivity apparently arises from the influence of the orientation about the glycosidic bond, which is anti for B, but syn for Z DNA.

Other modes with predominant imidazole ring character, as evidenced by ^{15}N or C8 ^{2}H shifts,[27] include prominent bands at 1339 and 1482 cm^{-1} for adenine, and at 1326 and 1489 cm^{-1} for guanine. Both purines show a strong band at ~1580 cm^{-1}, which is assigned to a mode based on the C2=N3—C4=C5—N7=C8 triene system. The guanine 1364-cm^{-1} band is also assigned to a triene mode, based on a vibronic coupling enhancement pattern (see below).

(25) Dollish, F. R.; Fateley, W. G.; Bentley, F. F. "Characteristic Raman Frequencies of Organic Compounds"; Wiley: New York, 1974.

(26) Delabar, J. M.; Majoube, M. *Spectrochim. Acta, Part A* **1978**, *34*, 129.

(27) (a) Lane, M. J.; Thomas, G. J., Jr. *Biochemistry* **1979**, *18*, 3839. (b) Livramento, J.; Thomas, G. J., Jr. *J. Am. Chem. Soc.* **1974**, *96*, 6529.

B. Enhancement Patterns. The enhancements of the RR bands are related to the normal mode compositions and to the excited-state bonding changes, as Peticolas and co-workers[18] have emphasized. For an allowed electronic transition, the scattering amplitude is given by Albrecht's A term:[28]

$$A = (M_e^0)^2 \frac{1}{\hbar} \sum_j \frac{\langle 1|j\rangle\langle j|0\rangle}{\nu_{j0} - \nu_e + i\Gamma_j} \quad (2)$$

where M_e^0 is the electronic transition dipole moment. If the displacement between the excited and ground state is small, the $|0\rangle$ and $|1\rangle$ levels dominate the sum over j, and the sum becomes proportional to Δ^e, the Franck-Condon overlap between vibrational levels $|0\rangle$ and $|1\rangle$ of the ground and excited state. (Note that if the displacement is zero, $\langle i|j\rangle = \delta_{ij}$, and the mode will be absent in the RR spectrum.) The RR intensity for the jth normal mode then becomes:

$$I_j = K(\Delta_j^e)^2\Omega_j^2 \quad (3)$$

where K is a constant for a given incident frequency and Ω_j is the frequency of the jth vibration. It can be easily shown that:[18]

$$\Delta_j^e = \sum_k L_{jk}^{-1}(-C_1)(\Delta b_{rs}^e) \quad (4)$$

where Δb_{rs}^e is the change in bond order between atoms r and s on going to excited state e, $(-C_1)$ is a constant 0.18 Å per unit bond order for both C–C and C–N bonds, and L_{jk} is the Wilson L matrix available from normal coordinate calculations. This leads to an equation in which the intensity of the RR band is proportional to the bond-order changes between the ground state and the excited state.

The allowed purine and pyrimidine transitions between 270 and 200 nm are π–π^* in character, and these are expected to provide most of the RR intensity, via the A term. The in-plane vibrational modes which should be enhanced are those involving stretching of ring and exocyclic bonds that experience the largest bond-order changes in the resonant excited states. Peticolas and co-workers[18] have shown that RR enhancements calculated with the aid of currently available normal coordinate analyses and CNDO-derived bond-order changes for the longest wavelength excited state of dUMP are in reasonable accord with experiment for some bands. However, major discrepancies were noted (vide infra), suggesting a need for better calculations of the gound- and/or excited-state potentials.

Not all the π–π^* transitions are stongly allowed, and some of them may give rise to vibronic coupling modes that mix in allowed character from nearby excitations. These modes are subject to enhancement via Albrecht's B term,[28] and may become prominent when the laser is resonant with the weakly allowed transition. An example of this mechanism is suggested below for dGMP. Also, the very weak n–π^* transitions, expected within the same wavelength region[30] may provide enhancement for out-of-plane vibrational modes, which are effective in mixing n–π^* with π–π^* states. This phenomenon has been well characterized for pyrazine.[31] Such modes could serve to identify n–π^* resonances, and also may be particularly sensitive to structural features of the nucleic acids, especially H-bonding.

In the ensuing discussion we examine the RR enhancements in the light of the experimental electronic transition wavelengths, intensities, and polarizations, as described by Callis[17] (Figure 3), the CNDO-derived transition monopoles for the π–π^* excitations, as discussed by Hug and Tinoco,[29] and the CNDO bond-order changes reported by Ziegler et al.[15]

1. dUMP and dTMP. Uracil and thymine have a single strong transition in their 265-nm absorption bands, polarized along the C4=O bond (Figure 3), and a second one, polarized perpendicular to the first, at 215 nm. Consistent with there being only two resonant transitions, we observe only two RR enhancement patterns (Figures 4 and 5). At 240 nm, the pattern is the same as at 266 nm, but the overall intensity is much lower since the 240-nm line is much farther from the 265-nm transition. Likewise, the 200-nm enhancement is similar to that observed at 218 nm, though weaker.

According to the CNDO calculations, the 265-nm transition is clearly associated with the enone system of uracil (Figure 2). Hug and Tinoco[29] calculate that the two lowest energy electronic transitions of uracil are both centered on the enone fragment, but the second is much weaker than the first. These are followed closely by a third predicted transition, with substantial intensity, which is centered on the C2=O bond. Experiments associate the last calculated transition with the observed 215-nm absorption band. It is therefore expected that excitation near 215-nm should preferentially enhance the C2=O stretch and modes coupled to it, whereas excitation near 265 nm should enhance modes coupled to the C5=C6—C4=O system. These expectations can be used to assign the observed RR bands of dUMP and dTMP in the double bond stretching region, 1600–1700 cm^{-1}, as described above.

At 218 nm the strongest band is at 1476 cm^{-1} for dUMP and 1484 cm^{-1} dTMP. The closest correspondence among the bands calculated by Tsuboi et al.[5] for 1-methyluracil at 1491 cm^{-1} has N1–C2 (38%) and C2–N3 stretching (17%) added out of phase. Though bond-order changes are expected in this region of the molecule, a larger change is calculated[15] along C2=O. A 1429-cm^{-1} uracil band calculated by Bowman and Spiro[32] to consist primarily of out-of-phase stretching of C2=O (25%) and N1—C2 (27%) is a preferred assignment, since a mode of this composition would have a particularly favorable overlap with the 215-nm excited state, based on the CNDO calculations.

The 1476-cm^{-1} band is weaker at 266 nm, where the transition is centered heavily on C5=C6.[29] For dUMP, the strongest band in the 266-nm spectrum is at 1230 cm^{-1}. None of the bands calculated for 1-methyluracil in this region involve any significant contribution from the stretching of the C6=C5—C4=O bonds, as would be implied by the very large enhancement, and by the disappearance of this band in the 218-nm spectrum. This discrepancy has been noted by Peticolas and co-workers,[18] who were unable to calculate any significant RR intensity in this region, and concluded that the normal coordinate calculations must be in error. This seems likely, in view of the complexity of the mode structure in this region, as noted in the assignment section. dTMP shows strong enhancement for a corresponding band at 1244 cm^{-1}, but some of the intensity is shared with the nearby 1185-cm^{-1} band.

The dUMP and dTMP ring breathing modes at 783–785 cm^{-1} are not expected to discriminate strongly among allowed π–π^* states; they are moderately enhanced at both 266 and 218 nm. Likewise, the dUMP 1394-cm^{-1} band, assigned by Nishimura et al.[9] to a bond-alternate mode of the ring is enhanced via both transitions. The corresponding dTMP band at 1379 cm^{-1}, however, is enhanced only via the 265-nm transition, implying pronounced localization of the mode along C6=C5—C4=O, as noted above.

2. dCMP. The electronic spectrum of cytosine is more complicated than that of uracil (Figure 3). Instead of just two strong transitions in the region of interest, there appear to be four of comparable intensity, at 270, 240, 215, and 205 nm. The four excitation wavelengths used in this study happen to be nearly coincident with each of these transitions. There are only three different enhancement patterns, however, the spectra at 240 and 218 nm resembling each other quite closely. Conceivably only one of these transitions is actually resonant, the other one being somehow ineffective in enhancing the Raman bands. In that case the spectrum at the wavelength of the inactive transition should be much weaker. For example, the dUMP RR spectrum is over four times weaker at 240 than at the resonant wavelength, 266 nm (Figure 4). The dCMP spectra at 240 and 218 nm are within a factor of 2 to 3 in intensity, and we tentatively conclude that

(28) Tang, J.; Albrecht, A. C. In "Raman Spectroscopy"; Szymanski, H. A., Ed.; Plenum Press: New York, 1970; Vol. 2, p 33.
(29) Hug, W.; Tinoco, I. *J. Am. Chem. Soc.* **1973**, *95*, 2803.
(30) Hug, W.; Tinoco, I. *J. Am. Chem. Soc.* **1974**, *96*, 665.
(31) (a) Ito, M.; Suzuka, I.; Udagawa, Y.; Kaya, K.; Mikami, N. *Chem. Phys. Lett.* **1972**, *16*, 211. (b) Kalantar, A. H.; Franzosa, E. S.; Innes, K. K. *Ibid.* **1972**, *17*, 335. (c) Kamagawa, K.; Ito, M. *J. Mol. Spectrosc.* **1976**, *60*, 277.
(32) Bowman, W. D.; Spiro, T. G. *J. Chem. Phys.* **1980**, *73*, 5482.

the two resonant transitions have similarly distorted excited states.

Comparison of the RR enhancements with the CNDO transition monopole patterns calculated for cytosine[29] is less informative than it is for uracil. The first three electronic transitions are calculated to involve the C6=C5—C4=N3 enamine fragment, with major contributions from the exocyclic C4—NH_2 and C2=O bonds in the second and third transitions, respectively.[29] The C2=O stretch, at 1652 cm^{-1}, is comparably enhanced, however, at all four wavelengths. The ~1237-cm^{-1} band assigned to C4-NH_2 stretching is seen only at 266 nm, suggesting a possible reversal of the first two transitions. Likewise, the 1605-cm^{-1} NH_2 scissors mode is seen more clearly at 266 than at 240 and 218 nm, and is most prominent at 200 nm. In this connection, we note the strong RR enhancement observed by Ziegler and Hudson[33] for the 958-cm^{-1} umbrella mode of ammonia upon excitation at 213 nm, in resonance with an excitation of the NH_3 lone pair. It is possible that the 205-nm transition involves a similar promotion of the NH_2 p electrons. This promotion may also be involved in the adenine and guanine transitions near 200 nm, since the NH_2 scissors modes of dAMP and dGMP are also prominent at this wavelength.

At all wavelengths except 200 nm the most prominent dCMP band is the one at 1528 cm^{-1}. This band is calculated[5] (1538 cm^{-1}) for 1-methylcytosine to involve mainly stretching of N3=C4, one of the double bonds in the enimine fragment. The other enimine double bond is C5=C6, which is calculated to contribute significantly (along with N1-C6) to a 1-methylcytosine mode at 1320 cm^{-1}. We associate this calculated mode with the 1294-cm^{-1} band seen strongly at 266 and 200 nm, and more weakly at the other two wavelengths. At 266 nm, another strong band is seen at 1250 cm^{-1}, which is absent in the remaining spectra. This mode probably has a composition similar to the 1230-cm^{-1} dUMP band, which dominates its 266-nm spectra, and is sensitive to N3 H/D exchange; no change in this band is observed for dCMP in D_2O (Figure 11) since in this case N3 is not protonated. The 782-cm^{-1} ring breathing mode is significantly enhanced at all four wavelengths, as expected.

3. dGMP. The electronic spectrum of guanine shows additional complexities. There are two electronic transitions contributing to the long-wavelength absorption band, at 255 and 275 nm, with long and short axis polarization, respectively (Figure 3). According to the CNDO calculations,[29] the 255-nm transition, designated I, is largely localized on the N7=C8 double bond of the imidazole ring, while the 275-nm transition, designated II, can be thought of as the lowest energy transition of the C2=N3—C4=C5—N7=C8 triene fragment. The 266-nm laser wavelength lies between these two transitions, both of which may be expected to contribute to the RR spectrum. Consistent with this is the strong enhancement for the two bands at 1489 and 1578 cm^{-1}. The 1489-cm^{-1} band is localized at the C8 region of the molecule as evidenced by its 28-cm^{-1} downshift upon the C8 deuteration;[27] we associate it with a mode calculated[5] at 1459 cm^{-1} for 9-methylguanine, which is a coupled motion of the N7=C8 and C8—N9 stretches and the C8—H bend. This mode should gain maximal enhancement via resonance with transition I (localized at N7=C8). On the other hand, the 1578-cm^{-1} band is calculated (at 1592 cm^{-1}) to consist of stretching of the central triene bond, C5=C4, out-of-phase with the flanking C4—N3 and C5—N7 bonds; this is precisely the mode expected to show greatest enhancement for transition II, in which the bond-order changes of the triene alternate in sign.

With 240-nm excitation, which is on the high-energy side of the composite absorption band, the 1489-cm^{-1} RR band retains greater intensity than the 1578-cm^{-1} band. Thus the 1489- and 1578-cm^{-1} bands are plausibly linked to the 255- and 275-nm electronic transitions, respectively, in conformity with the relative ordering of transitions I and II from the CNDO calculations. Likewise a band at 1326 cm^{-1} is enhanced in parallel with the 1489-cm^{-1} band, and is also localized at the C8 region, as shown by its 17-cm^{-1} downshift upon C8 deuteration.[27]

(33) Ziegler, L. D.; Hudson, B. *J. Phys. Chem.* **1984**, *88*, 1110.

At 218 nm excitation is in resonance with a weak electronic transition of guanine (Figure 3), calculated[29] to be the second triene-based transition, designated III. In a symmetric triene, this transition would be electric dipole forbidden. The RR spectrum is dominated by a single intense band at 1364 cm^{-1}. Since the resonant electronic transition is weak, we infer that this band gains its enhancement via a vibronic *B* term mechanism,[28] by mixing the quasi-forbidden triene transition with the fully allowed higher lying transitions. Examination of the coupling matrix elements between the second triene transition and allowed triene transitions suggests that the most effective mixing mode would involve stretching of the triene bonds in the following phase: +C8=N7 + N7—C5 - C4—N3 - N3=C2. Unfortunately, no mode with this pattern can be found in the list of calculated frequencies for 9-methylguanine.[5] Both ends of the triene are clearly involved in the mode since the frequency is lowered in D_2O and also upon ^{15}N substitution in the imidazole[26] ring or binding of *cis*-dichlorodiammineplatinum(II) at N7.[15] The normal mode calculation should be reexamined with respect to this assignment. It is also of interest that the C6=O stretch, at 1679 cm^{-1}, gains appreciable enhancement at 218 nm, as noted by Ziegler et al.[15] for 213-nm excitation. This is consistent with a significant monopole at the C6 oxygen atom in transition III.[29]

At shorter wavelengths, the guanine absorption rises into a strong band, which is again a composite of two electronic transitions, at 205 and 190 nm, polarized along the long and short axes of the molecule, respectively (Figure 3). The calculated fourth transition, IV, is delocalized over both rings.[29] Similar enhancement is seen for many modes at 200 and 266 nm, and the triene-based modes at 1364 and 1578 cm^{-1} are prominent. Strong enhancement is also seen for the C6=O stretch at 1679 cm^{-1}, even though no significant contribution from this part of the molecule is indicated by the transition IV monopoles. It seems likely that this enhancement arises from the fifth transition, at 190 nm, which is polarized along the C6=O direction. As mentioned above, the prominence of the 1603-cm^{-1} NH_2 mode suggests involvement of the NH_2 p electrons in at least one of the short-wavelength transitions.

4. dAMP. The first four calculated electronic transitions of adenine[29] are similar to those of guanine. Transition I, which is localized on the N7=C8 bond, is at lowest energy, while the next two transitions, which are associated with the triene pathway, are both quite weak. In conformity with this expected pattern, a strong short axis polarized transition is observed at 260 nm, followed by two weak transitions at 245 and 230 nm (Figure 3). With 266-nm excitation prominent RR bands are seen (Figure 8) at 1339 and 1482 cm^{-1}, which are localized at the C8 end of the molecule (see assignments in Table II), consistent with the dominance of transition I in the resonance scattering. Appreciable enhancement is also seen for the 1604-cm^{-1} NH_2 mode, and for a band at 1581 cm^{-1}, which can be associated, as in guanine, with the triene pathway. At 240 nm, which lies between the two weak electronic transitions, the RR enhancement pattern is considerably weaker. The 1482- and 1581-cm^{-1} bands drop in intensity by a factor of about 6 and 4, respectively, while the 1339-cm^{-1} band is reduced by a factor of 10. This result is consistent with the energy ordering of transitions I and II being reversed with respect to guanine.[17]

At shorter wavelengths, adenine has another strong absorption band, with two equally strong transitions, at 213 and 200 nm, polarized along the long and short molecular axes, respectively (Figure 3). The 218- and 200-nm laser lines are essentially coincident with these two transitions, and the overall enhancements are comparable. In both cases the 1582-cm^{-1} band, associated with the triene pathway,[34] is dominant, while the C8-localized modes at 1482 and 1339 cm^{-1} are less strongly enhanced (although a 1423-cm^{-1} band, which is also sensitive to C8 deuteration (Table

(34) Adenine is the one nucleic acid base that retains an aromatic ring from its parent purine structure. Thus, the 1582-cm^{-1} vibration may be related in character to the ν_{8a} ring mode of substituted benzenes which show similar enhancement with 213-nm excitation via vibronic coupling in benzenoid excited states. This type of mode is not calculated in the normal coordinate analysis.

II), is enhanced at 200 nm). At 218 nm, the 730-cm^{-1} band, seen weakly at other wavelengths, gains special prominence; this is assigned as a deformation mode of the imidazole ring.[5] At 200 nm, the 1604-cm^{-1} NH_2 band is strongly enhanced, consistent with the polarization of the resonant transition, along the C6–NH_2 bond; as suggested above for dCMP and dGMP, the NH_2 p electrons may be especially important in this transition.

5. Summary. Many features of the RR enhancement pattern for the purines and pyrimidines can be understood on the basis of the currently available normal mode and π–π^* transition moment analyses, but other pieces of the puzzle do not yet fit. The purine spectra are consistent with the expected dominance of a N7=C8 localized transition in the ~270-nm absorption band, and with a distribution of delocalized triene-based transitions at long and short wavelengths. For guanine, there is evidence for vibronic mixing of the second, quasi-forbidden triene state with the allowed ones. For uracil and thymine, the expected dominance at long and short wavelengths of transitions involving the C6=C5—C4=O and C2=O fragments, respectively, is borne out by the observed enhancement pattern. The importance of the strong band at 1230 (dUMP) or 1244 cm^{-1} (dTMP) in the long-wavelength spectra suggests a need for revising the normal coordinate calculations. For cytosine, there does not appear to be any clear correlation of the enhancements with the CNDO-derived bond-order changes. A point of considerable interest is the strong enhancement at 200 nm for the NH_2 scissors mode of cytosine, adenine, and guanine, which suggests an important role for the NH_2 p electrons in the excited states occurring in this region.

C. Wavelength Selectivity among the Bases. A major impediment to the application of nonresonance (or preresonance) Raman spectroscopy to the investigation of naturally occurring nucleic acids has been the problem of overlapping contributions from different bases. The spectra are crowded and many of the ring modes of different bases are in sufficiently close proximity that the individual bands cannot be resolved. The dramatically altered enhancement patterns observed at the different UV wavelengths offer promise for overcoming this problem via variable-wavelength excitation of nucleic acid spectra. To illustrate the possibilities, we recorded RR spectra at each of the four UV wavelengths for equimolar mixtures of dTMP, dCMP, dAMP, and dGMP. These are shown in Figure 14, along with an identification of the major contributors to each of the observed bands, as inferred from the overall enhancements relative to the ~3400-cm^{-1} H_2O band.

The C=O stretching bands of dCMP (1652 cm^{-1}) and dTMP (1655 cm^{-1}) are overlapped, but the intensity for T is ca. three times greater than C at 266 nm, whereas the ratio is similar at 240 and 218 nm; at 200 nm, the intensities are reversed. Thus one would use 266- and 200-nm excitation, respectively, to monitor the C=O frequencies of T and C. The C=O bond of G, at 1679 cm^{-1}, is weak at all wavelengths, but does show up as a shoulder at 200 nm. These C=O stretches are of great interest in connection with H-bond effects in nucleic acids. The NH_2 scissors modes can likewise be expected to be directly influenced by H-bonding, but the frequencies are essentially the same, 1604 ± 1 cm^{-1}, for C, G, and A, making identification problematical. The enhancement values show that G is by far the dominant contributor at 240 nm. A does not dominate at any wavelength, but its contribution is comparable to G at 266 nm, which are both ~10-fold stronger than C. A comparison of the 266- and 240-nm spectra could be used to isolate the A and G contributions.

The 1578- and 1581-cm^{-1} triene modes of G and A are overlapped, but the A intensity exceeds the G intensity by a factor of ~3 at 218 nm, while the intensities are similar at 266, 240, and 200 nm. The band at 1482–1489 cm^{-1} contains contributions from G and A (C8-localized modes at 1489 and 1482) and also T (C2=O coupled mode, at 1482 cm^{-1}). The dominant contributors are A at 266 nm (by factors of ~1.5 and ~13 over G and T), G at 240 (by factors of ~2 and ~15 over A and T), and T at 218 nm (by factors of ~4 and ~6 over A and G); at 200 nm the A and G contributions are comparable, and about twice as strong as that of T. The 1528-cm^{-1} band of C stands out clearly from all other contributions and is particularly prominent at 218 nm. The entire 1290–1390-cm^{-1} region of the spectrum is badly crowded, but the 1339- and 1379-cm^{-1} A and T bands are seen clearly at 266 nm, excitation at 218 nm brings out the 1309- and 1364-cm^{-1} bands of A and G, while the 1294-cm^{-1} C band is uniquely prominent at 200 nm.

C and T have ring modes at 782 and 785 cm^{-1}, but the C contribution is dominant (factor of 2 or greater) at all wavelengths except 240 nm where the contributions are equal. Excitation at 218 nm brings out the 730-cm^{-1} imidazole ring deformation of A particularly clearly. The important 679-cm^{-1} G mode, which is a marker for the B → Z conformational transition of $(dG\text{-}dC)_n$ sequences,[7] is rather weak at all wavelengths, but can be brought out clearly by suitable amplification at 218 or 200 nm.

These enhancement factors cannot be applied directly to nucleic acid duplexes, because they are expected to be affected rather strongly by base pairing and stacking interactions. Nevertheless, it appears quite likely that selective excitation at the available UV wavelengths can be used to advantage in isolating most of the bands of interest for the individual bases.

Conclusions

1. Good-quality UV RR spectra of the nucleotides can be obtained with 266-, 240-, 218-, and 200-nm excitation, using the YAG laser and H_2 Raman shifter. They show vibrational modes of the purine and pyrimidine bases, with dramatic variations in the enhancement pattern at the different wavelengths.
2. These enhancement variations are helpful in resolving overlapped modes and making vibrational assignments.
3. Many features of the RR enhancement are explicable from the excited-state distortions expected on the basis of CNDO calculations, but some features are discrepant and imply a need for better vibrational or electronic calculations, or both.
4. The observed enhancement patterns hold out promise for resolving the contributions from the individual bases to nucleic acid Raman spectra, using variable-wavelength excitation.

Acknowledgment. We thank Professors Hudson and Peticolas for sending us a copy of their nucleotide paper prior to publication. This work was supported by NIH Grant GM25158 and a NSF grant. R.P.R. is the recipient of a postdoctoral research fellowship, No. NIH 5 F32 GM 09104-02.

Registry No. dUMP, 964-26-1; dTMP, 365-07-1; dCMP, 1032-65-1; dGMP, 902-04-5; dAMP, 653-63-4.